Kasner eons in Lovelock black holes

Pablo Bueno,[*] Pablo A. Cano,[†] Robie A. Hennigar,[‡] and Ming-Da Li[§]

Departament de Física Quàntica i Astrofísica, Institut de Ciències del Cosmos, Universitat de Barcelona, Martí i Franquès 1, E-08028 Barcelona, Spain

(Received 29 September 2024; accepted 15 November 2024; published 6 December 2024)

In the vicinity of spacelike singularities, general relativity predicts that the metric behaves, at each point, as a Kasner space which undergoes a series of "Kasner epochs" and "eras" characterized by certain transition rules. The period during which this process takes place defines a "Kasner eon," which comes to an end when higher-curvature or quantum effects become relevant. When higher-curvature densities are included in the action, spacetime can undergo transitions into additional Kasner eons. During each eon, the metric behaves locally as a Kasner solution to the higher-curvature density controlling the dynamics. In this paper we identify the presence of Kasner eons in the interior of static and spherically symmetric Lovelock gravity black holes. We determine the conditions under which eons occur and study the Kasner metrics which characterize them, as well as the transitions between them. We show that the null energy condition implies a monotonicity property for the effective Kasner exponent at the end of the Einsteinian eon. We also characterize the Kasner solutions of more general higher-curvature theories of gravity. In particular, we observe that the Einstein gravity condition that the sum of the Kasner exponents adds up to 1, $\sum_{i=1}^{D-1} p_i = 1$, admits a universal generalization in the form of a family of Kasner metrics satisfying $\sum_{i=1}^{D-1} p_i = 2n - 1$ which exists for any order-n higher-curvature density and in general dimensions.

DOI: 10.1103/PhysRevD.110.124015

I. INTRODUCTION

Curvature singularities occur ubiquitously in general relativity, both in cosmology and in black holes [1]. They represent a complete breakdown of the classical theory and mark the limits of its predictive power. It is commonly thought that quantum gravity will resolve singularities, but very little is known about this in practice. What is certain is that quantum effects will play an essential role near singularities, and understanding these effects along with how, if, or what kinds of singularities can be resolved are fundamentally important questions.

A remarkable fact is that the "death throes" of general relativity contain a very universal structure. As shown by Belinski, Khalatnikov, and Lifshitz (BKL), general relativity admits generic spacelike singularities that are ultralocal and oscillatory, characterized by an infinite sequence of Kasner epochs and eras [2]. Importantly, the onset of BKL dynamics can occur already at curvature scales where the classical theory should remain reliable. These universal features may provide a path to understand quantum effects on singularities.

In the approach to a spacelike singularity, there is a decoupling of spatial points, leading to an emergent ultralocality where each spatial point evolves independently from the others. In this regime, the universe is described by a generalized Kasner metric, which is similar to the familiar Kasner solution,

$$\mathrm{d}s^2 = -\mathrm{d}t^2 + \sum_{i=1}^{(D-1)} t^{2p_i}\mathrm{d}x_i^2, \qquad \sum_{i=1}^{(D-1)} p_i = \sum_{i=1}^{(D-1)} p_i^2 = 1, \tag{1.1}$$

with the difference being that the exponents p_i are permitted to depend on space. The corresponding period of time where the generalized Kasner metric remains a good approximation is known as a Kasner epoch. The ultralocal regime is punctuated by brief transitions driven by spatial curvature wherein the universe transitions from one Kasner epoch to another. Kasner eras comprise larger time intervals and are made up of several epochs. The defining feature of an era is that the transitions between epochs involve the repeated swapping of the smallest two Kasner exponents while the remaining exponents monotonically decrease. The sequence of transitions, and the corresponding changes in expansion and contraction of the

[*]Contact author: pablobueno@ub.edu
[†]Contact author: pablo.cano@icc.ub.edu
[‡]Contact author: robie.hennigar@icc.ub.edu
[§]Contact author: limd23@icc.ub.edu

universe, leads to the oscillatory dynamics in the approach to the singularity.

One manifestation of quantum gravitational effects, common to many approaches, is the appearance of higher-derivative corrections to the Einstein-Hilbert action [3–9]. In the approach to a singularity, these terms will ultimately become important and will lead to drastic modifications of the BKL analysis. While there has been growing interesting in understanding aspects of the black hole interior and singularity, e.g., Refs. [10–19], there have been very few studies concerning the implications of higher-curvature corrections for ultralocality and the chaotic, oscillatory dynamics predicted by BKL.[1] It was recently argued by three of us that the consideration of higher-derivative corrections naturally introduces the concept of an eon: periods which are dominated by emergent physics at each energy scale [23]. From this perspective, the period in which the entire BKL dynamics of general relativity occurs constitutes the Einsteinian eon. Different ways by which the Einsteinian eon may come to an end were explored in [23], including the possibility of finite volume singularities, inner horizons, or additional eons.

It was proposed in [23] that under certain circumstances, such as a hierarchy of energy scales, additional eons could appear. During the additional eons, one could imagine modified BKL-like dynamics, consisting of epochs and eras, but with the Kasner exponents obeying modified constraints and transition rules dictated by the modified gravitational equations. Exploring this idea concretely is a rather difficult but interesting problem requiring the extension of the BKL analysis to higher-curvature theories of gravity. As evidence for this idea, a toy model was explored, consisting of the interior of a spherically symmetric black hole in Gauss-Bonnet gravity. The Gauss-Bonnet theory introduces a new energy scale by its coupling constant λ. For scales $M \gg r \gg \sqrt{\lambda}$, it was observed that the interior geometry is given, to a good approximation, by a Kasner solution of Einstein gravity. However, for $r \ll \sqrt{\lambda}$, a transition occurs, and the geometry is then given by a Kasner solution of the Gauss-Bonnet theory—this is a Gauss-Bonnet eon consisting of a single Kasner epoch. The interior solution provides a smooth connection between the Einsteinian and Gauss-Bonnet eons.

The purpose of this paper is to further explore the ideas of [23] as a step toward a more complete understanding of how higher-curvature corrections alter and supplement the results of the BKL analysis. We begin in Sec. II by performing a classification of Kasner solutions of various higher-curvature theories. We point out an apparently universal feature, namely, that for every density involving n powers of the Riemann tensor, there exists a family of Kasner solutions for which the sum of the Kasner exponents equals $2n-1$, generalizing the Einstein gravity result. Then, in Sec. III, we focus on Lovelock theory where analytical black hole solutions are available, and we study the Kasner geometries that emerge in the black hole interior. Introducing an effective Kasner exponent which is constant during periods where the metric is approximately Kasner, we study the existence of eons in these black holes, illustrating how the Einsteinian eon can be followed either by additional Lovelock eons or terminate in a finite volume singularity.[2] Finally, in Sec. IV, we make some more general remarks concerning the end of an eon. We derive perturbative formulas governing the behavior of the effective Kasner exponent at the end of an eon, which connects our results with the more traditional effective field theory program. Finally, we show that if the effective stress tensor generated by the higher-curvature terms respects the null energy condition, then the effective Kasner exponent exhibits a monotonic behavior at the end of the Einsteinian eon. In Appendix, we perform a detailed analysis of the different types of interiors which arise as a function of the sign and magnitude of the gravitational couplings for Gauss-Bonnet gravity in general dimensions as well as for cubic Lovelock gravity in $D = 7$.

II. KASNER SOLUTIONS IN HIGHER-CURVATURE GRAVITY

We are interested in Kasner solutions to higher-curvature theories of gravity.[3] The Kasner metric is given by (1.1), and the equations of motion of a given theory constrain the "Kasner exponents" p_i in different ways. In order to characterize such constraints, it is convenient to introduce the parameters μ, ν, as

$$\mu \equiv \sum_{i=1}^{(D-1)} p_i, \qquad \nu \equiv \sum_{i=1}^{(D-1)} p_i^2. \tag{2.1}$$

These are invariant under arbitrary permutations of pairs of Kasner exponents. In the case of Einstein gravity,

[1]Much of this work has focused on developing singularity probes, i.e., identifying holographic observables that are sensitive to the behavior of the black hole interior. Among such approaches, one (which we shall return to in the conclusions of our work) is holographic complexity [20–22], which posits a connection between the time-dependent dynamics of the black hole interior and the growth of circuit complexity for the dual CFT state in the case of asymptotically anti–de Sitter black holes. Here, our focus will be primarily on asymptotically flat black holes, but in the conclusions, we shall make some comments on the anti–de Sitter case.

[2]Therefore, in this paper, we do not focus on the cases in which the higher-curvature terms give rise to additional inner horizons. In that context, it has recently been shown that adding infinite towers of higher-curvature corrections can lead to a full resolution of the Schwarzschild black hole singularity in $D \geq 5$ [24–28].

[3]For other examples of investigations of Kasner solutions for specific higher-curvature theories, see, e.g., Refs. [29–32].

$$I = \int \mathrm{d}^D x \sqrt{|g|} R, \tag{2.2}$$

there exists a $(D-3)$-parametric family of solutions determined by the conditions

$$\mu = 1, \qquad \nu = 1. \tag{2.3}$$

Additionally, there exists an isolated solution corresponding to $p_1 = p_2 = \ldots = p_{(D-1)} = 0$, which is nothing but D-dimensional Minkowski spacetime.

We are interested in Kasner solutions of the form (1.1). In order to find solutions of this type, one can insert an ansatz of the above form in the corresponding equations of motion and find the conditions for the Kasner exponents. Alternatively, we can consider an ansatz with D arbitrary functions of the form

$$\mathrm{d}s^2 = -N(t)\mathrm{d}t^2 + \sum_{i=1}^{(D-1)} a_i(t)\mathrm{d}x_i^2, \tag{2.4}$$

find the on-shell action

$$S[N, a_i] \equiv \int \mathrm{d}t L[N, a_i],$$
$$\text{where } L[N, a_i] \equiv \sqrt{N(t)a_1(t)\cdots a_{D-1}(t)}\mathcal{L}|_{(2.4)}, \tag{2.5}$$

and vary it with respect to those functions. The result reads

$$\frac{N^2}{\sqrt{N a_1 \cdots a_{D-1}}}\frac{\delta S[N, a_i]}{\delta N} = \mathcal{E}_{tt}[N, a_i],$$
$$-\frac{a_i^2}{\sqrt{N a_1 \cdots a_{D-1}}}\frac{\delta S[N, a_i]}{\delta a_i} = \mathcal{E}_{ii}[N, a_i], \tag{2.6}$$

where $\mathcal{E}_{ab}[N, a_i] \equiv \frac{1}{\sqrt{|g|}}\frac{\delta S}{\delta g^{ab}}\Big|_{(2.4)}$ are the field equations of the theory evaluated on the ansatz (2.4). Hence, solving the Euler-Lagrange equations of the effective Lagrangian associated with $N(t)$ and $a_i(t)$ is equivalent to solving the full nonlinear equations of motion—see, e.g., Refs. [33–37] for previous instances in which similar methods were used for finding solutions with different isometries. Once we have the equations, we can set $N(t) = 1$, $a_i(t) = t^{2p_i}$, and solve them for p_i.

A. A universal feature

In the following subsections, we use the above method to characterize the Kasner metrics of various higher-curvature theories in the absence of matter. Our list if not fully exhaustive as, in certain cases, there exist isolated sets of solutions which cannot be easily characterized in general dimensions and for arbitrary curvature orders. Additionally, for a given curvature order, one can either study the Kasner solutions for general values of the coupling constants or, alternatively, study the solutions of isolated densities. The first approach gives rise to very messy expressions as soon as we move beyond quadratic curvature order. Just like for Einstein gravity, in each case, we find the existence of broad families of solutions, corresponding to hypersurfaces in the $\{p_i\}_{i=1,\ldots,D-1}$ hyperplane characterized by certain constraints on the values of μ and ν, as well as sets of isolated solutions which correspond to points in such a hyperplane.

Our analysis reveals an interesting general feature. Namely, we observe that the family of metrics characterized by the Einsteinian conditions (2.3) gets generalized, for general order-n densities,

$$I = \int \mathrm{d}^D x \sqrt{|g|}\mathrm{Riem}^n, \tag{2.7}$$

to a family of solutions characterized by a condition of the form

$$\mu = 2n - 1, \tag{2.8}$$

plus an additional, more complicated constraint which can be written in the form

$$\nu = \nu(\{\alpha_i\}, p_3, p_4, \ldots, p_{(D-1)}), \tag{2.9}$$

where ν is, in general, a complicated function of the relative gravitational couplings α_i and $(D-3)$ of the Kasner exponents. Therefore, we find that μ does not depend on the spacetime dimension, and its dependence on the order of the density is a remarkably simple generalization of the Einstein gravity case, corresponding to $\mu = 1$. We have verified this feature for $f(R)$, quadratic, cubic, and Lovelock gravities in various dimensions, which makes us confident that this is indeed a universal property of higher-curvature densities. It is then more than tempting to conjecture that by assuming some generalized BKL-type behavior persists in the interior of generic black holes dominated by higher-curvature interactions, the corresponding Kasner exponents characterizing the spacetime metric at each point will satisfy (2.8) and (2.9) instead of the usual conditions (2.3).

B. Explicit examples

1. $f(R)$ gravity

Consider a density consisting of an arbitrary power of the Ricci scalar, namely,

$$I = \int \mathrm{d}^D x \sqrt{|g|} R^n. \tag{2.10}$$

Interestingly, whenever $n \geq 2$, this theory admits Kasner solutions whose exponents satisfy a single relation

(instead of two), namely,

$$\nu = \mu(2-\mu), \tag{2.11}$$

where μ can, in principle, take any real value, but it is constrained to the range $0 \leq \mu \leq 2$ in order for the metric to remain real valued. In D dimensions, this represents a $(D-2)$-parametric family of solutions. This obviously includes the Einstein gravity set (2.3) as well as Minkowski as particular cases. In addition to this family, there exist "isolated" solutions corresponding to

$$p_1 = p_2 = \cdots = p_{(D-1)} = -\frac{(2n-1)(n-1)}{\left(n-\frac{D}{2}\right)}, \tag{2.12}$$

for every D and $n \neq D/2$.

2. Quadratic gravities

The next natural case corresponds to general quadratic gravity of the form

$$I = \int \mathrm{d}^D x \sqrt{|g|}[\alpha_1 R^2 + \alpha_2 R_{ab}R^{ab} + \alpha_3 R_{abcd}R^{abcd}]. \tag{2.13}$$

This theory admits a new $(D-3)$-parametric family of solutions satisfying $\mu = 3$ in general dimensions. In $D = 4$, this satisfies

$$\mu = 3, \qquad \nu = \frac{-3\alpha_1 + \alpha_2 + 7\alpha_3 \pm 2\sqrt{2}\sqrt{-(\alpha_2+4\alpha_3)(3\alpha_1+\alpha_2+\alpha_3)}}{\alpha_1+\alpha_2+3\alpha_3}. \tag{2.14}$$

In order for the solutions to exist, ν must be real and positive, which imposes the conditions

$$\left\{\alpha_2 < -4\alpha_3, -\frac{1}{3}(\alpha_2+\alpha_3) \leq \alpha_1 < -(\alpha_2+3\alpha_3)\right\} \tag{2.15}$$

or, alternatively,

$$\left\{\alpha_2 > -4\alpha_3, -(\alpha_2+3\alpha_3) < \alpha_1 \leq -\frac{1}{3}(\alpha_2+\alpha_3)\right\}. \tag{2.16}$$

As a consequence, setting any pair of couplings to zero gives rise to invalid solutions. For instance, if we choose $\alpha_2 = -4\alpha_3$, which would put the action in the form of a linear combination of R^2 with the Gauss-Bonnet density, one would get $\nu = -3$, which is not allowed. In addition, setting $\alpha_1 = \alpha_3 = 0$, which would be a pure $R_{ab}R^{ab}$ theory, would yield $\nu = 1 + 2\mathrm{i}\sqrt{2}$, and $\alpha_1 = \alpha_2 = 0$ would give $\nu = \frac{1}{3}[7 + 4\mathrm{i}\sqrt{2}]$, which is not valid either. On the other hand, the combination $\alpha_2 = -3\alpha_1 - \alpha_3$, which corresponds to a linear combination of a Weyl tensor-squared term plus a $R_{abcd}R^{abcd} - R_{ab}R^{ab}$ one, produces a valid result, namely, $\nu = 3$. In the $D = 4$ case, the general quadratic theory also admits a family of solutions of the same type as Einstein gravity, namely, satisfying (2.3). In addition, there is an isolated solution corresponding to

$$p_1 = p_2 = p_3 = \frac{1}{2}. \tag{2.17}$$

In higher dimensions, the expression for ν gets increasingly complicated. For instance, the $D = 5$ version of (2.14) reads

$$\mu = 3, \qquad \nu = \frac{-3\alpha_1 + \alpha_2 + 7\alpha_3 - 2\alpha_3 p_3 p_4 \pm \frac{1}{2}\sqrt{A(\alpha_1,\alpha_2,\alpha_3,p_3,p_4)}}{\alpha_1+\alpha_2+3\alpha_3}, \tag{2.18}$$

where

$$\begin{aligned} &A(\alpha_1,\alpha_2,\alpha_3,p_3,p_4) \\ &\equiv \left[6\alpha_1 - 2\left(\alpha_2 + \alpha_3(7-2p_3p_4)\right)\right]^2 - 4(\alpha_1+\alpha_2+3\alpha_3) \\ &\quad \times \left[9\alpha_1 + 9\alpha_2 + \alpha_3\left(27 - 4p_3p_4(2(p_3p_4 \right.\right. \\ &\quad \left.\left. + (p_3-3)p_3 + p_4^2) - 6p_4 + 9)\right)\right], \end{aligned} \tag{2.19}$$

and where we chose to write p_1 and p_2 in terms of μ, ν. For $D \geq 5$, the Einstein gravity family (2.3) is no longer a solution. On the other hand, there exist additional isolated solutions satisfying $p_1 = p_2 = \cdots = p_{(D-1)}$ for certain dimension-dependent combinations of α_1, α_2, α_3.

3. Cubic gravities

The most general cubic Lagrangian contains eight independent densities built from contractions of the Riemann tensor and the metric—see, e.g., Ref. [38]. In this case, the expressions are rather messy already in $D = 4$ and not particularly illuminating. However, we find that in all cases there exists a family of solutions characterized by the conditions

$$\mu = 5, \quad \nu = \nu(\{\alpha_i\}, p_3, p_4, \ldots, p_{(D-1)}), \tag{2.20}$$

again in agreement with our general observation.

4. Lovelock gravities

Consider now the case of Lagrangians consisting of a Lovelock density of curvature order n. The action is given by

$$I = \int_{\mathcal{M}} \mathrm{d}^D x \sqrt{|g|} \mathcal{X}_{2n}, \tag{2.21}$$

where the dimensionally extended Euler densities $\mathcal{X}_{2n}$ are given by[4]

$$\mathcal{X}_{2n} = \frac{1}{2^n} \delta^{\mu_1 \ldots \mu_{2n}}_{\nu_1 \ldots \nu_{2n}} R^{\nu_1 \nu_2}_{\mu_1 \mu_2} \ldots R^{\nu_{2n-1} \nu_{2n}}_{\mu_{2n-1} \mu_{2n}}. \tag{2.22}$$

The simplest instance beyond the Einstein-Hilbert term corresponds to the Gauss-Bonnet density, which reads

$$\mathcal{X}_2 = R^2 - 4 R_{ab} R^{ab} + R_{abcd} R^{abcd}. \tag{2.23}$$

This term contributes nontrivially to the equations of motion for $D \geq 5$. In particular, for $D = 5$, we find a family of Kasner solutions characterized by the conditions

$$\mu = 3, \qquad p_1 = 0, \tag{2.24}$$

where one of the Kasner exponents vanishes and the others are free provided the first condition holds. Moving on to $D = 6$, we find the families

$$\mu = 3, \qquad p_1 = p_2 = 0, \tag{2.25}$$

$$\mu = 3, \qquad \sum_{i=1}^{5} \frac{1}{p_i} = 0. \tag{2.26}$$

All of these families were previously identified in [39], where an exhaustive classification of the Kasner solutions of Lovelock densities in the particular cases of curvature orders satisfying $D = 2n + 1$ and $D = 2n + 2$ was performed. Moving on to $D = 7$, we find a family of solutions characterized by

$$\mu = 3, \qquad \nu = \nu(p_3, p_4, p_5), \tag{2.27}$$

where

$$\begin{aligned}
\nu(p_3, p_4, p_5) \equiv & \big[2p_3^3(p_4 + p_5 + p_6) + 2p_3^2(p_4 + p_5 + p_6 - 3)(p_4 + p_5 + p_6) + p_3(p_4 + p_5 + p_6) \\
& \times \big(2(p_4^2 + p_4(p_5 + p_6 - 3) + p_5^2 + p_5 p_6 + p_6^2) - 6p_5 - 6p_6 + 9\big) \\
& + 2p_4^3(p_5 + p_6) + 2p_4^2(p_5 + p_6 - 3)(p_5 + p_6) + p_4(p_5 + p_6) \\
& \times \big(2(p_5 p_6 + (p_5 - 3)p_5 + p_6^2) - 6p_6 + 9\big) + p_5 p_6 \big(2(p_5 p_6 + (p_5 - 3)p_5 + p_6^2) - 6p_6 + 9\big)\big] \\
& \times \big[p_3(p_4 + p_5 + p_6) + p_4(p_5 + p_6) + p_5 p_6\big]^{-1}.
\end{aligned}$$

Interestingly, all the above solutions reduce to the class

$$\mu = 3, \qquad \nu = 1 + \frac{8}{(D-1)}, \tag{2.28}$$

when $p_2 = \cdots = p_{D-1} = 4/(D-1)$, a case which will be relevant in the analysis of spherically symmetric black hole interiors.

Moving to the case of the cubic Lovelock density, we find for $D = 7$ the family of solutions

$$\mu = 5, \qquad p_1 = 0, \tag{2.29}$$

whereas for $D = 8$,

$$\mu = 5, \qquad p_1 = p_2 = 0, \tag{2.30}$$

$$\mu = 5, \qquad \sum_{i=1}^{7} \frac{1}{p_i} = 0. \tag{2.31}$$

In both cases, these were previously identified in [39]. In $D = 9$, one finds a family of solutions analogous to (2.27) but with

$$\mu = 5, \quad \nu = \nu(p_3, p_4, p_5, p_6, p_7) \tag{2.32}$$

and where $\nu(p_3, p_4, p_5, p_6, p_7)$ is not a very illuminating function. Again, in all cases, the solutions reduce to a class characterized by

$$\mu = 5, \quad \nu = 1 + \frac{24}{(D-1)}, \tag{2.33}$$

when $p_2 = \cdots = p_{D-1} = 6/(D-1)$.

Both (2.28) and (2.33) are particular instances of a more general class of solutions to a general Lovelock density $\mathcal{X}_{2n}$ and in general dimensions, in the particular case in which all exponents but one are equal. This corresponds to

$$\mu = 2n - 1, \quad \nu = 1 + \frac{4n(n-1)}{(D-1)}, \tag{2.34}$$

where

[4]The generalized Kronecker symbol is defined as $\delta^{\mu_1 \mu_2 \ldots \mu_r}_{\nu_1 \nu_2 \ldots \nu_r} \equiv r! \delta^{[\mu_1}_{\nu_1} \delta^{\mu_2}_{\nu_2} \ldots \delta^{\mu_r]}_{\nu_r}$.

$$p_1 = -\frac{(D-2n-1)}{(D-1)}, \quad p_2 = \cdots = p_{D-1} = \frac{2n}{(D-1)}. \tag{2.35}$$

We will see in the following section that this family of solutions arises approximately during certain periods as the singularity of static and spherically symmetric Lovelock black holes is approached.

III. KASNER EONS FROM BLACK HOLE INTERIORS

In this section, we consider static and spherically symmetric black hole solutions of Lovelock gravity. As the singularity is approached, those spacetimes undergo one or several Kasner eons through which they locally behave like Kasner solutions of the corresponding higher-curvature density. In the first subsection, we define an effective Kasner exponent which becomes constant during an eon for a general static and spherically symmetric spacetime. Then, we use this notion to characterize the presence of Kasner eons in the interior of Lovelock gravity black holes. We determine the conditions under which, depending on the sign and magnitude of the gravitational couplings, the Einsteinian eon is followed by additional higher-curvature eons or terminates in a finite-volume singularity.

A. Effective Kasner exponents

In this section, we focus on the case in which all but one of the exponents coincide with each other, namely, when

$$p_1 \neq p_2 = p_3 = \cdots = p_{D-1}. \tag{3.1}$$

Very often, the metric which describes the near-singularity region of static black hole solutions of higher-curvature theories takes the form (1.1), with Kasner exponents satisfying this condition. Indeed, consider a general static and spherically symmetric black hole with a single horizon, a spacelike curvature singularity at $r = 0$, and an interior metric described in Schwarzschild coordinates as

$$ds^2 = \frac{dr^2}{f(r)} - N(r)f(r)dz^2 + r^2 d\Omega^2_{(D-2)}, \tag{3.2}$$

where $d\Omega^2_{(D-2)}$ is the metric of the $(D-2)$-dimensional sphere, and where the two functions $f(r)$ and $N(r)$ behave as

$$f(r) \overset{r\to 0}{\sim} -r^{-s}, \qquad N(r) \overset{r\to 0}{\sim} r^{-w} \tag{3.3}$$

near the singularity, which lies in the future of any infalling observer. Changing coordinates

$$d\tau \equiv \frac{dr}{\sqrt{-f}} \Rightarrow \tau \sim r^{(s+2)/2}, \tag{3.4}$$

the metric becomes

$$ds^2 = -d\tau^2 + \tau^{2p_1} dz^2 + \tau^{2p_2} d\Omega^2_{(D-2)}, \tag{3.5}$$

where the two independent exponents read

$$p_1 = -\frac{(s+w)}{(s+2)}, \quad p_2 = \frac{2}{(s+2)}. \tag{3.6}$$

Hence, in the vicinity of any point of the $(D-2)$-sphere, the metric takes the usual Kasner form[5]

$$ds^2 = -d\tau^2 + \tau^{2p_1} dz^2 + \sum_{i=2}^{(D-1)} \tau^{2p_i} dx_i^2, \tag{3.7}$$

where (3.6) holds and

$$p_2 = p_3 = \cdots = p_{D-1}. \tag{3.8}$$

In such a general situation, the sums of the Kasner exponents and their squares, as defined in (2.1), become

$$\mu = \frac{2(D-2)-(s+w)}{(s+2)}, \quad \nu = \frac{4(D-2)+(s+w)^2}{(s+2)^2}. \tag{3.9}$$

We can introduce an "effective" Kasner exponent $p_{\rm eff}$ for the dz^2 component of the metric,

$$p_{\rm eff}(r) \equiv \frac{r[f(r)N(r)]'}{[2f(r) - rf'(r)]N(r)}, \tag{3.10}$$

so that any time that $f(r) \sim r^{-s}, N(r) \sim r^{-w}$, $p_{\rm eff}(r)$ becomes constant, the metric is locally Kasner, and

$$p_1 = p_{\rm eff}, \quad p_2 = \cdots = p_{D-1} = p_{\rm eff} + 1 + \frac{w}{(s+2)}. \tag{3.11}$$

In the present context, Kasner eons correspond to periods during which the interiors of black holes in the vicinity of spacelike singularities behave as locally Kasner metrics with approximately constant Kasner exponents satisfying (3.11). As we will see below, for solutions involving several parametrically distinct length scales, as the singularity is approached, the solutions will transit through various eons characterized by different exponents.

The above expressions get considerably simplified for black holes characterized by a single metric function, namely, those for which $N(r) = 1$. In that case, whenever $f(r) \sim r^{-s}$, eons are characterized by Kasner exponents satisfying the conditions

[5]Strictly speaking, the interior belongs to the class of Kantowski-Sachs cosmological models, which have $\mathbb{R} \times \mathbb{S}^2$ spatial sections. However, locally, in the vicinity of any point on the two-sphere, the metric can be brought into the usual Kasner form.

$$p_1 = p_{\rm eff} = -\frac{s}{(s+2)},$$
$$p_2 = \cdots = p_{D-1} = p_{\rm eff} + 1 = \frac{2}{(s+2)}. \tag{3.12}$$

Consider, for instance, the case of the D-dimensional Schwarzschild black hole, whose metric function reads

$$f(r) = 1 - \frac{r_0^{D-3}}{r^{D-3}}, \tag{3.13}$$

where r_0 is an integration constant related to the mass of the solution M via

$$r_0^{D-3} = \frac{16\pi G M}{(D-2)\Omega_{D-2}}, \tag{3.14}$$

where Ω_{D-2} is the (dimensionless) volume of the transverse $(D-2)$-sphere. In this case, the effective Kasner exponent reads

$$p_{\rm eff}(r) = -\frac{D-3}{(D-1)-2u^{D-3}}, \qquad u \equiv r/r_0. \tag{3.15}$$

For $u \ll 1$—namely, near the singularity—this approaches a constant,

$$p_{\rm eff} = -\frac{(D-3)}{(D-1)}, \tag{3.16}$$

and the metric locally behaves like a Kasner spacetime with exponents

$$p_1 = -\frac{(D-3)}{(D-1)}, \qquad p_2 = \cdots = p_{D-1} = \frac{2}{(D-1)}, \tag{3.17}$$

which satisfy $\mu = \nu = 1$, as expected for Einstein gravity.

B. Lovelock gravity black holes

Now, let us consider the case of a general Lovelock gravity in D dimensions. The action is given by

$$I = \int_{\mathcal{M}} {\rm d}^D x \sqrt{|g|}\mathcal{L}_{\rm Lovelock}, \tag{3.18}$$

where

$$\mathcal{L}_{\rm Lovelock} \equiv \frac{1}{16\pi G}\left[R + \sum_{n=2}^{\lfloor (D-1)/2 \rfloor} \lambda_n \frac{(D-2n-1)!}{(D-3)!}\mathcal{X}_{2n}\right] \tag{3.19}$$

is the Lovelock Lagrangian [40,41] and where we set the cosmological constant to zero. The dimensionally extended Euler densities $\mathcal{X}_{2n}$ are defined in (2.22), and the λ_n are arbitrary coupling constants with dimensions of length$^{2(n-1)}$.

Static, spherically symmetric black holes in Lovelock theory take the form (3.2) with $N(r) = 1$, where the function $f(r)$ satisfies the algebraic equation

$$h(\psi) = \frac{r_0^{D-3}}{r^{D-1}}, \quad \text{where } \psi \equiv \frac{1 - f(r)}{r^2}, \tag{3.20}$$

and where the "characteristic polynomial" $h(x)$ is given by [42–46]

$$h(x) \equiv x + \sum_{n=2}^{\lfloor (D-1)/2 \rfloor} \lambda_n x^n. \tag{3.21}$$

Equation (3.20) has n solutions for $f(r)$. Of those, only one reduces, in each case, to the Schwarzschild one in the limit in which $\lambda_n \to 0 \quad \forall\ n$, and we will exclusively consider that case from now on. Then, the interior of a Lovelock black hole can be more complicated than in Einstein gravity. For example, even in the absence of charge or rotation, it is possible to have an inner Cauchy horizon. Moreover, Lovelock black holes can have what are known as "branch singularities," which occur when a root of the polynomial $h(x)$ has a branch point [47,48]. While the metric remains finite, the radial derivatives of the metric function blow up at a branch singularity, meaning this is also a curvature singularity with a divergent Kretschmann scalar. The volume of spatial slices does not become arbitrarily small at a branch singularity—rather, it remains finite. A thorough analysis of the different types of interiors which arise as a function of the sign and magnitude of the gravitational couplings is presented in Appendix for Gauss-Bonnet gravity in general dimensions as well as for cubic Lovelock gravity in $D = 7$—namely, in the cases in which the Lovelock series is truncated at quadratic and cubic orders, respectively.

Let us consider first the case in which the black holes contain a singularity at $r = 0$. This is generically the case if $\text{sign}(\lambda_n) = + \forall\ n$. In the deep interior of such a black hole, it is only the highest-order density that contributes to the field equation. A simple computation shows that these Lovelock black holes have Kasner regimes in the deep interior which precisely correspond to the class of pure Kasner solutions of Lovelock gravity identified in (2.34) and (2.35). In particular, note that those relations, combined with the fact that for Lovelock theory we must have $n \leq (D-1)/2$, imply the following bounds on the Kasner exponents, in general:

$$-1 \leq p_1 \leq 0, \qquad 0 \leq p_{i\geq 2} \leq 1. \tag{3.22}$$

For $D = 5$ and $D = 6$, the Einsteinian eon—characterized by approximately constant effective Kasner exponents with values given by (3.17)—is terminated when the

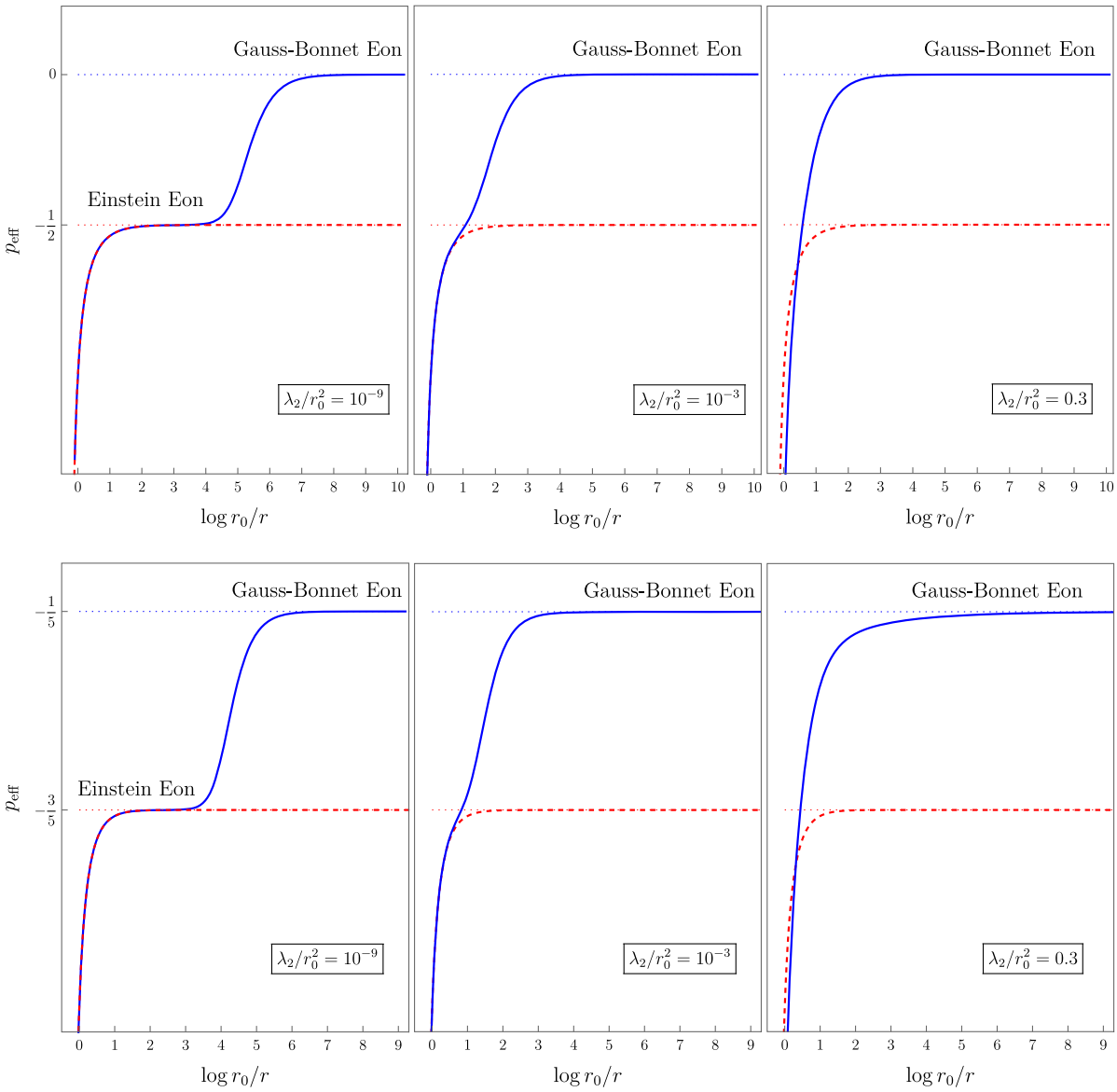

FIG. 1. Effective Kasner exponent for Lovelock gravity black holes in $D = 5$ (upper row) and $D = 6$ (lower row) for various values of the Gauss-Bonnet coupling. For sufficiently small values of λ_2/r_0^2, the metric undergoes a Kasner eon characterized by the Einstein gravity exponent $p_{\rm eff} = -(D-3)/(D-1)$ and then transits to a new eon controlled by the Gauss-Bonnet density with $p_{\rm eff} = -(D-5)/(D-1)$ which characterizes the near-singularity metric. The dashed red curve corresponds to the usual D-dimensional Schwarzschild black hole.

Gauss-Bonnet term becomes dominant, and the effective Kasner exponents transition to approximately constant values given by (2.35) with $n = 2$. If λ_2 is large enough, we can completely skip the Einsteinian eon, with $p_{\rm eff}$ transitioning directly to the Gauss-Bonnet phase. More precisely, if λ_2 is such that there exists a regime for which

$$|\lambda_2|/r_0^2 \ll u^{D-1} \ll 1, \tag{3.23}$$

then there will be an Einsteinian eon corresponding to values of r for which the above condition holds. On the other hand, if u^{D-1} becomes of the same order as $|\lambda_2|/r_0^2$ before $u^{D-1} \ll 1$ holds, the Einsteinian eon will be skipped, and the transition will be directly to the Gauss-Bonnet one. These different cases are shown in particular examples for $D = 5$ and $D = 6$ in Fig. 1.

For $D \geq 7$, the last eon corresponds to (2.35) with $n = \lfloor (D-1)/2 \rfloor$, and additional intermediate eons may arise (or be absent altogether) depending on the relative strength of the couplings. In case they arise, during each of those intermediate eons, Eq. (2.35) holds, with n corresponding to the order of the density which dominates the dynamics throughout that phase. The situation in which all possible intermediate eons arise requires that (3.23) holds

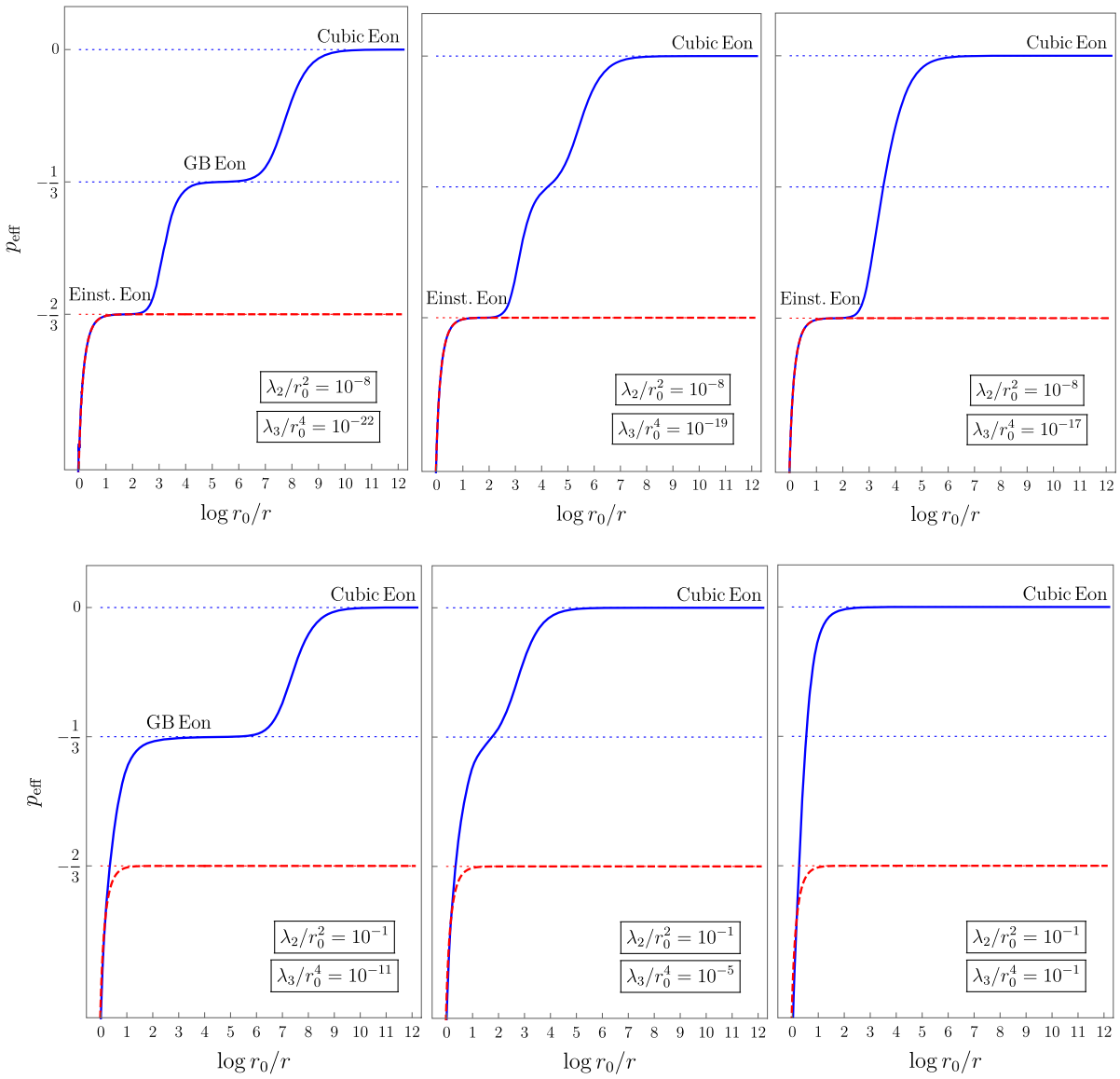

FIG. 2. Effective Kasner exponent for Lovelock gravity black holes in $D = 7$. Depending on the values of $|\lambda_3|/r_0^4$ and $|\lambda_2|/r_0^2$, it is possible to have three eons (upper left), an Einsteinian eon followed by a cubic Lovelock eon (upper right), a Gauss-Bonnet eon followed by a cubic Lovelock eon (lower left), or a single cubic Lovelock eon (lower right). The dashed red curve corresponds to the seven-dimensional Schwarzschild black hole.

for certain u and that there exists a hierarchy of couplings of the form

$$|\lambda_n|^{1/(2(n-1))} \ll \cdots \ll |\lambda_3|^{1/4} \ll |\lambda_2|^{1/2}. \quad (3.24)$$

The various situations arising in the $D = 7$ case are shown in Fig. 2.

The cases considered so far are such that the effective Kasner exponent increases monotonically until it reaches a plateau corresponding to the final eon. However, for $D \geq 7$, it is possible to have transitions between eons which involve a nonmonotonic behavior of $p_{\rm eff}$ and still conclude with a final eon which extends all the way to a singularity at $r = 0$. For instance, this occurs in $D = 7$ for $\lambda_2 < 0$, $1 > \lambda_3/r_0^4 > \lambda_2^2/(3r_0^4)$, as shown in some examples in Fig. 3.

We mentioned earlier that finite-volume singularities generically occur for Lovelock black holes for certain combinations of the couplings. In that case, an Einsteinian eon can still be present in the interior for sufficiently small values of the higher-curvature couplings. The radial derivative of the metric function $f(r)$ diverges at the finite-volume singularity, which we take to be at $r = r_\star$. Comparing with (3.10), it follows that

$$\lim_{r\to r_\star} f'(r) = \infty \Rightarrow p_{\rm eff}(r_\star) = -1. \quad (3.25)$$

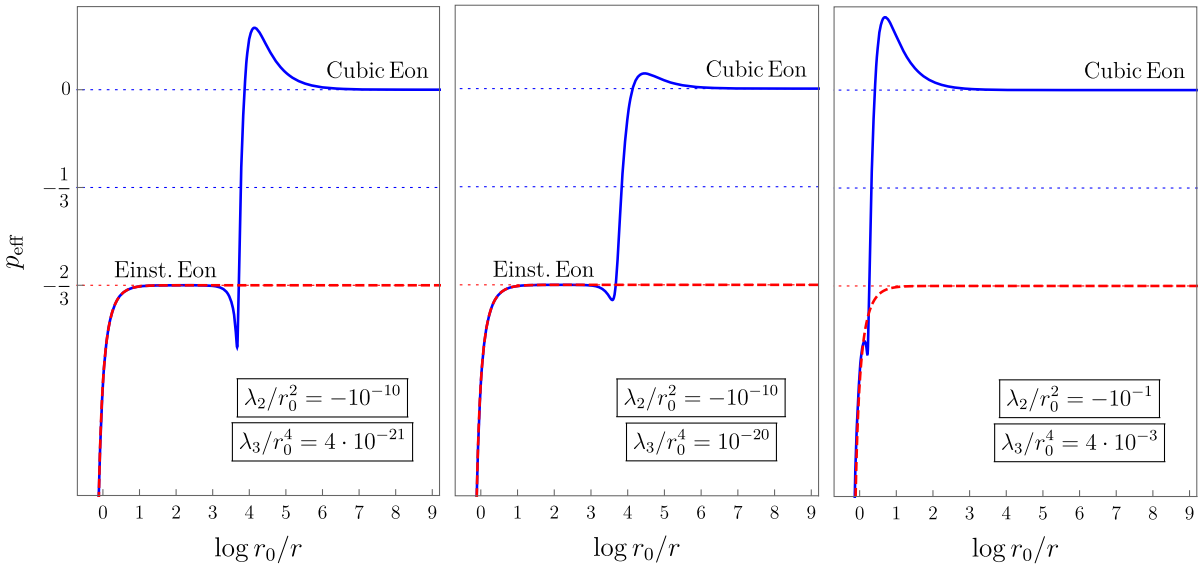

FIG. 3. Effective Kasner exponent for Lovelock gravity black holes in $D = 7$ for certain combinations of λ_2, λ_3 which give rise to a nonmonotonic behavior of $p_{\rm eff}$.

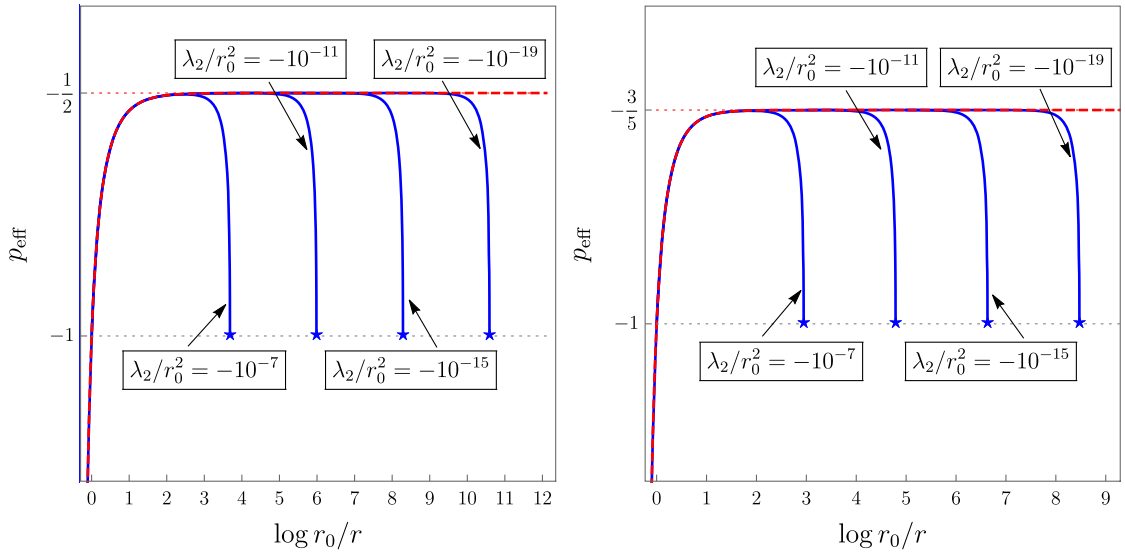

FIG. 4. Effective Kasner exponent for Lovelock gravity black holes in $D = 5$ (left) and $D = 6$ (right) for various negative values of the Gauss-Bonnet coupling. For sufficiently small values of $|\lambda_2|/r_0^2$, an Einsteinian eon is present. Eventually, the effective Kasner exponent starts decreasing and takes the value $p_{\rm eff} = -1$ at the branch singularity $r = r_\star \equiv (4|\lambda_2|/r_0^2)^{1/(D-1)}$.

Hence, in this case, the Einsteinian eon is followed by a decrease in $p_{\rm eff}$ which terminates at the singularity, where it takes the value -1 for general theories and dimensions. Examples of this behavior are shown in Fig. 4.

IV. END OF AN EON

In this section, we take a closer look at how a Kasner eon comes to an end. We provide a perturbative formula for the effective Kasner exponent at the end of a Lovelock gravity eon and make some general comments about the termination of the Einsteinian one. In addition, we show that if the effective stress tensor generated by higher-curvature terms satisfies the null energy condition, then the effective Kasner exponent exhibits a monotonic behavior at the end of the Einsteinian eon.

A. End of an eon in Lovelock theory

As we have seen, during an eon, the effective Kasner exponent is approximately constant. However, if higher-curvature terms are present, then eventually these will

become important and drive the universe to a new eon, as shown in the figures above. In Lovelock theory, we can analytically derive the leading corrections to $p_{\rm eff}$ in that regime.

Since it is easy to do so, let us consider the following situation. The universe is in an eon where the Lovelock term of order n dominates. We consider a transition between the order n eon and an order m eon. The coupling λ_n is treated nonperturbatively, while we compute only the leading correction for λ_m. The result of this computation is

$$p_{\rm eff} = -\frac{D-2n-1}{D-1} + \frac{2(m-n)}{D-1}\frac{|\lambda_m| u^{(D-1)(1-m/n)}}{|\lambda_n|^{m/n} r_0^{2(m/n-1)}} + \cdots . \tag{4.1}$$

An eon can be considered to have ended when the second term in the above equation becomes $\mathcal{O}(1)$, which happens at the point where

$$\frac{|\lambda_m| u^{(D-1)(1-m/n)}}{|\lambda_n|^{m/n} r_0^{2(m/n-1)}} \sim 1. \tag{4.2}$$

Naturally, the most interesting case is the end of the Einstein gravity eon (this is also the case that is within reach of conventional effective field theory). Thus, we consider the case where $n = 1$ and allow m to remain arbitrary. It is convenient to introduce a scale ℓ for the coupling λ_m so that $\lambda_m \sim \mu_m \ell^{2m-2}$ where μ_m is dimensionless and order one and ℓ is a length scale. The result is that the Einstein eon ends at

$$r_{\rm end} \sim r_0 \left(\frac{\ell}{r_0}\right)^{2/(D-1)}, \tag{4.3}$$

which is independent of m. In other words, the result is the same whether it is Gauss-Bonnet gravity or the 12th-order Lovelock gravity that takes over. Notably, because of the fractional exponent $2/(D-1)$, this point can be orders of magnitude larger than the length scale ℓ that characterizes the new physics.[6] The result is more intuitive when expressed in terms of the proper time. Since the proper time during the Einstein gravity eon is

$$\tau \sim r_0 u^{(D-1)/2}, \tag{4.4}$$

we have $\tau_{\rm end} \sim \ell$.

B. Monotonicity of the effective Kasner exponent

In the examples we have studied, we have seen that the effective Kasner exponent often—but not always—increases as one moves toward the singularity. Moreover, we saw that the finite volume singularities were always associated with an effective Kasner exponent that decreases at the end of an eon. Here, we place these observations on a somewhat more rigorous footing, making a connection between the monotonicity of the effective Kasner exponent and the null energy condition.

The null energy condition requires that $T_{\mu\nu}k^\mu k^\nu \geq 0$ for all null vectors k. Here, we are considering vacuum spacetimes of higher-curvature theories. While, strictly speaking, there is no matter in the setup, we can consider the higher-curvature terms to generate an effective stress-energy tensor $T_{\mu\nu} = G_{\mu\nu}$. For a static and spherically symmetric spacetime characterized by a single metric function $f(r)$, the null energy condition implies the following constraint:

$$G_{\mu\nu}k^\mu k^\nu \geq 0 \quad \forall k^\mu \Rightarrow r^2 f'' + (D-4) r f' + 2(D-3)(1-f) \geq 0. \tag{4.5}$$

Let us now study the end of the Einsteinian eon. Consider a correction of the form

$$f(r) = 1 - \left(\frac{r_0}{r}\right)^{D-3} + \lambda \left(\frac{r_0}{r}\right)^{s}, \tag{4.6}$$

where λ is a coupling parameter and $s > D-3$ so that the correction is subleading to the Einstein terms. We are considering this not as an exact solution but instead as a model of the leading (in λ) correction to the Schwarzschild solution. Plugging this into the constraint above, we find

$$r^2 f'' + (D-4) r f' + 2(D-3)(1-f) = \lambda (s-2)(s-D+3) \left(\frac{r_0}{r}\right)^{s}, \tag{4.7}$$

indicating that the null energy condition is satisfied provided that $\lambda > 0$.

Next, consider the derivative of the effective Kasner exponent at the end of the Einsteinian eon. Expanding to leading order in λ and working in the $r \ll r_0$ limit, we find

$$p'_{\rm eff}(r) = -\frac{2\lambda (s-D+3)^2}{r_0 (D-1)^2} \left(\frac{r_0}{r}\right)^{D-4-s}. \tag{4.8}$$

To make the result more transparent and consistent with the plots, let us introduce the coordinate $y \equiv \log(r_0/r)$ which increases toward the singularity. In terms of this coordinate, we obtain

$$\frac{dp_{\rm eff}}{dy} = \frac{2\lambda (s+D-3)^2}{(D-1)^2} e^{(s-D+3)y}. \tag{4.9}$$

This means that if the null energy condition is satisfied, then the effective Kasner exponent must increase at the end

[6] This feature has been emphasized in [49,50].

of the Einsteinian eon. On the other hand, if the effective Kasner exponent is seen to *decrease* toward the singularity, then this indicates a violation of the null energy condition. This latter result was seen to be universally associated with the finite volume singularities of Gauss-Bonnet gravity studied in the earlier sections—see Fig. 4.

The effective Kasner exponent is negative in Einstein gravity and governs the expansion of spacetime along the z direction in the black hole interior. The above result tells us that if the corrections to general relativity respect the null energy condition, then this expansion slows down as a result of the corrections. Of course, it is worth pointing out that quantum effects *can* lead to violations of the null energy condition. A proper analysis should invoke instead the achronal averaged null energy condition [51]. However, this analysis is beyond the scope of the present work, and the null energy condition itself can still serve as a useful heuristic.

A natural question is whether the null energy condition can tell us anything about the monotonicity of the p_{eff} at the end of other Lovelock eons beyond the Einsteinian one. Unfortunately, the answer appears to be no. It would be interesting to assess whether other constraints can yield useful insights in this case.

V. DISCUSSION

Motivated by the key role they play in the approach to a spacelike singularity, we began our work by classifying the types of Kasner solutions that can arise in higher-curvature theories of gravity. In general, the conditions on the Kasner exponents differ significantly from Einstein gravity. We noted a universal feature of Kasner metrics in higher-curvature gravity: For a theory incorporating n powers of curvature, there always exists a Kasner solution for which the exponents satisfy

$$\sum_{i=1}^{D-1} p_i = 2n - 1. \tag{5.1}$$

In the case of Einstein gravity, $n = 1$ and the well-known condition on the sum of the Kasner exponents is recovered. For general relativity, the above is the unique condition on the sum of the Kasner exponents dictated by the field equations. However, in higher-curvature theories, there can be additional families of solutions beyond this universal one. It is nonetheless natural to speculate that the Einstein gravity condition $\sum_{i=1}^{D-1} p_i(x) = 1$, satisfied at each spatial point in the approach to a generic singularity, would be replaced by (5.1) with spatially dependent exponents in the case of Kasner eons dominated by order-n densities. This would rely on the persistence of ultralocality in those cases, a feature which remains to be explored.

We have further explored the concept of a Kasner eon first introduced in [23], focusing on the example of Lovelock gravity. We have provided a detailed analysis of the interior structure of Lovelock black holes and analyzed examples where additional eons or finite volume singularities occur in the interior. A key result of our analysis concerns the monotonicity of the effective Kasner exponent at the end of the Einsteinian eon. We demonstrated that if the effective stress tensor generated by the higher-curvature corrections obeys the null energy condition, then the effective Kasner exponent must increase at the end of the Einsteinian eon. Since this exponent (when negative) controls the expanding direction of the universe, the physical implication is that the null energy condition demands that the expansion in this direction *slows* as the singularity is approached. The net result is that, very close to the singularity, the spatial volume of the universe collapses more slowly, scaling like

$$V \sim \tau^{1+\delta(D-1)}, \qquad p_{\text{eff}} = -\frac{(D-3)}{(D-1)} + \delta. \tag{5.2}$$

Going forward, it will be important to understand the holographic implications of Kasner eons. Here, we have focused on the asymptotically flat setting, but our results will carry over to the asymptotically AdS case as well. This is because, in the deep black hole interior, the negative cosmological constant becomes irrelevant. As one example, the existence of eons can explain the confusion that originally arose concerning applications of the "Complexity = Action" proposal [22] to higher-curvature black holes. It was observed that, even when the higher-curvature couplings are turned off, the late-time growth rate of complexity does not reduce to its Einstein gravity value [52–54]. Ultimately, this is because the late-time growth rate of complexity is sensitive to the final eon in the black hole interior. In fact, the late-time complexity growth rate in Lovelock theory (in $D > 2n + 1$) can be expressed in terms of the effective Kasner exponent [55],

$$\lim_{t\to\infty} \frac{d\mathcal{C}}{dt} = \frac{(D-1)(1+p_{\text{eff}})M}{\pi(D-2+(D-1)p_{\text{eff}})}. \tag{5.3}$$

Therefore, because the exponents governing the final eon in Lovelock theory are different from Einstein gravity, the growth rate is different. In addition, because the Kasner exponents are always constants independent of the couplings, the limit of the growth rate does not recover the Einstein gravity result. Substituting $p_{\text{eff}} = -(D-3)/(D-1)$ into the above, one recovers the well-known $2M/\pi$ predicted by general relativity. Further noting that the null energy condition requires that p_{eff} should increase at the end of the Einsteinian eon, one concludes that the complexification rate should decrease as additional eons are probed. It would be particularly interesting to revisit this analysis, considering, for example, the time dependence of complexity

which may exhibit distinct features as the Wheeler-DeWitt patch picks up contributions from different eons.

The interiors of spherically symmetric black holes provide a simple consistency check of the concept of eons. This is because one often has access to the exact solution. However, it will be important to test the concept of an eon under less symmetric conditions. Ultimately, the idea is that one may have additional BKL-like phases of evolution driven by higher-curvature or quantum corrections to the Einstein equations. It is therefore essential to explore these ideas as generically as possible without becoming too reliant on highly symmetric examples. We hope to return to this problem in the near future.

Note added. Recently, Ref. [56] appeared on the arXiv. That paper develops the ideas of Kasner eons in a manner complementary to our own, by exploring the role of matter and focusing on the case of quasitopological gravities. The authors also perform a preliminary investigation of the holographic interpretation of Kasner eons.

ACKNOWLEDGMENTS

We are grateful to Ángel Murcia and Yoav Zigdon for helpful comments and discussions. P. B. was supported by a Ramón y Cajal fellowship (RYC2020-028756-I) from Spain's Ministry of Science and Innovation and by Grant No. PID2022-136224NB-C22, funded by MCIN/AEI/10.13039/501100011033/FEDER, UE. P. A. C. received support from a fellowship from "la Caixa" Foundation (ID No. 100010434) with code LCF/BQ/PI23/11970032. R. A. H. received the support of a fellowship from "la Caixa" Foundation (ID No. 100010434) and from the European Union's Horizon 2020 research and innovation program under the Marie Skłodowska-Curie Grant Agreement No. 847648 under fellowship code LCF/BQ/PI21/11830027. M. D. L. was supported by a Chinese Scholarship Council (CSC) fellowship.

DATA AVAILABILITY

No data were created or analyzed in this study.

APPENDIX: INTERIOR OF LOVELOCK BLACK HOLES

1. Gauss-Bonnet in general D

Truncating the Lovelock action at quadratic order yields the Einstein-Gauss-Bonnet action

$$I=\frac{1}{16\pi G}\int_{\mathcal{M}}\mathrm{d}^{D}x\sqrt{|g|}\Big[R+\frac{\lambda_2}{(D-3)(D-4)}\times\left(R^2-4R_{ab}R^{ab}+R_{abcd}R^{abcd}\right)\Big], \tag{A1}$$

where again we set the cosmological constant to zero and λ_2 has dimensions of length^2. The Gauss-Bonnet term is dynamical for $D\geq 5$, topological in $D=4$, and trivially zero for $D\leq 3$.

In $D\geq 5$, the theory admits static and spherically symmetric black hole solutions characterized by a single metric function which satisfies

$$h(\psi)=\frac{r_0^{D-3}}{r^{D-1}},\quad \text{where } \psi\equiv\frac{1-f(r)}{r^2}. \tag{A2}$$

We always assume $r_0>0$, and the characteristic polynomial $h(x)$ is given by

$$h(x)\equiv x+\lambda_2 x^2. \tag{A3}$$

This equation has two solutions. We consider the one which has a well-defined Einstein-gravity limit when $\lambda_2/r_0^2\to 0$. This reads

$$f(r)=1+\frac{r^2}{2\lambda_2}\left[1-\sqrt{1+\frac{4\lambda_2 r_0^{D-3}}{r^{D-1}}}\right]\overset{(\lambda_2/r_0^2\to 0)}{=}1-\left(\frac{r_0}{r}\right)^{D-3}+\left(\frac{r_0}{r}\right)^{2(D-2)}\left(\frac{\lambda_2}{r_0^2}\right)+\ldots. \tag{A4}$$

Whenever

$$0\leq\left(\frac{\lambda_2}{r_0^2}\right)<1,\quad (D=5), \tag{A5}$$

$$0\leq\left(\frac{\lambda_2}{r_0^2}\right),\quad (D\geq 6), \tag{A6}$$

this function has a single real zero, $f(r_{\mathrm{h}})=0$, $r_{\mathrm{h}}>0$. In all such cases, the solution describes a black hole with a curvature singularity at $r=0$ hidden behind an event horizon at $r=r_{\mathrm{h}}$. The explicit form of r_{h} for the first few dimensions reads

$$r_{\mathrm{h}}=\sqrt{1-\left(\frac{\lambda_2}{r_0^2}\right)}\qquad (D=5), \tag{A7}$$

$$r_{\mathrm{h}}=\frac{\left[9+\sqrt{3}\sqrt{27+4\left(\frac{\lambda_2}{r_0^2}\right)^3}\right]^{1/3}}{2^{1/3}3^{2/3}}-\frac{2^{1/3}\left(\frac{\lambda_2}{r_0^2}\right)}{3^{1/3}\left[9+\sqrt{3}\sqrt{27+4\left(\frac{\lambda_2}{r_0^2}\right)^3}\right]^{1/3}}\qquad (D=6), \tag{A8}$$

$$r_{\mathrm{h}}=\frac{1}{\sqrt{2}}\sqrt{-\left(\frac{\lambda_2}{r_0^2}\right)+\sqrt{4+\left(\frac{\lambda_2}{r_0^2}\right)^2}}\qquad (D=7). \tag{A9}$$

On the other hand, in general $D \geq 5$, whenever

$$-\frac{1}{2^{\frac{D-5}{D-3}}} < \left(\frac{\lambda_2}{r_0^2}\right) < 0, \tag{A10}$$

the solution describes a black hole hidden behind an event horizon at $r = r_{\rm h}$, which has a finite-volume singularity at

$$r_\star \equiv \left(\frac{4|\lambda_2|}{r_0^2}\right)^{\frac{1}{D-1}}. \tag{A11}$$

Finally, whenever

$$\left(\frac{\lambda_2}{r_0^2}\right) \leq -\frac{1}{2^{\frac{D-5}{D-3}}}, \tag{A12}$$

the solution describes a naked singularity at $r_\star$. Additionally, in the special case of $D = 5$, a naked singularity at $r = 0$ also arises for

$$1 \leq \left(\frac{\lambda_2}{r_0^2}\right). \tag{A13}$$

2. Cubic Lovelock in $D = 7$

Consider now the case of a cubic Lovelock theory in $D = 7$. The Lagrangian reads

$$I = \frac{1}{16\pi G}\int_{\mathcal{M}} \mathrm{d}^7x\sqrt{|g|}\left[R + \frac{\lambda_2}{12}\mathcal{X}_4 + \frac{\lambda_3}{24}\mathcal{X}_6\right], \tag{A14}$$

where λ_2 and λ_3 have dimensions of length^2 and length^4, respectively. The theory admits static and spherically symmetric black hole solutions characterized by a single metric function which now satisfies

$$h(\psi) = \frac{r_0^4}{r^6}, \quad \text{where } \psi \equiv \frac{1 - f(r)}{r^2}, \tag{A15}$$

and where the characteristic polynomial $h(x)$ is now given by

$$h(x) \equiv x + \lambda_2 x^2 + \lambda_3 x^3. \tag{A16}$$

This equation has three solutions, which can be written as

$$f_A \equiv \frac{1}{3\lambda_3}\left[(3\lambda_3 + \lambda_2 r^2) + \frac{2^{1/3} r^4 (3\lambda_3 - \lambda_2^2)}{(\Sigma + 3\sqrt{3}\sqrt{\Upsilon})^{1/3}} - \frac{(\Sigma + 3\sqrt{3}\sqrt{\Upsilon})^{1/3}}{2^{1/3}}\right], \tag{A17}$$

$$f_B \equiv \frac{1}{3\lambda_3}\left[(3\lambda_3 + \lambda_2 r^2) - \frac{(1 + \mathrm{i}\sqrt{3}) r^4 (3\lambda_3 - \lambda_2^2)}{2^{2/3}(\Sigma + 3\sqrt{3}\sqrt{\Upsilon})^{1/3}} + \frac{(1 - \mathrm{i}\sqrt{3})(\Sigma + 3\sqrt{3}\sqrt{\Upsilon})^{1/3}}{2^{4/3}}\right], \tag{A18}$$

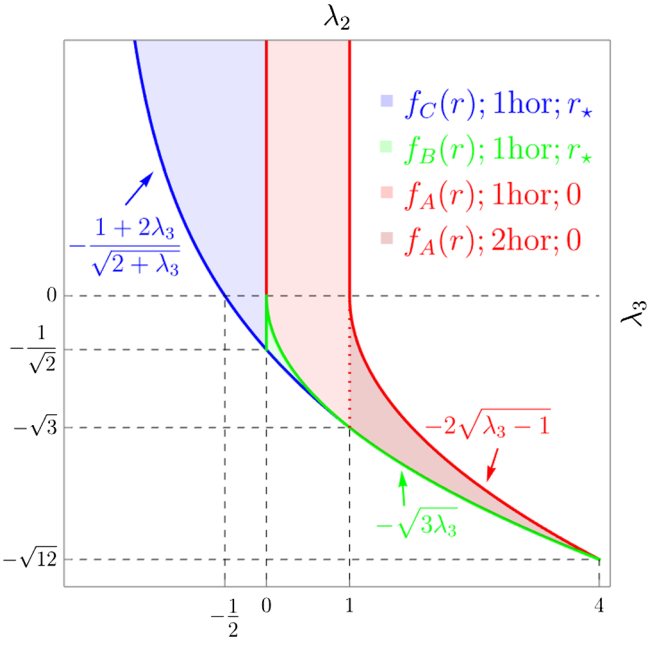

FIG. 5. Space of black hole solutions of the cubic Lovelock gravity with Lagrangian (A14) parametrized by the values of λ_2/r_0^2 and λ_3/r_0^4 (we omit r_0 everywhere to avoid the clutter). The blue region corresponds to black holes described by $f_C(r)$ and corresponds to black holes with a single horizon and with a finite-volume singularity at $r_\star$. The green region corresponds to black holes whose metric function is $f_B(r)$ and which possess a single horizon and a finite-volume singularity at $r_\star$. The lighter red region corresponds to black holes with a metric function given by $f_A(r)$ which possess a single horizon and a singularity at $r = 0$. Finally, the darker red region also contains black holes described by $f_A(r)$ with a singularity at $r = 0$ but with two horizons.

$$f_C \equiv \frac{1}{3\lambda_3}\left[(3\lambda_3 + \lambda_2 r^2) - \frac{(1 - \mathrm{i}\sqrt{3}) r^4 (3\lambda_3 - \lambda_2^2)}{2^{2/3}(\Sigma + 3\sqrt{3}\sqrt{\Upsilon})^{1/3}} + \frac{(1 + \mathrm{i}\sqrt{3})(\Sigma + 3\sqrt{3}\sqrt{\Upsilon})^{1/3}}{2^{4/3}}\right], \tag{A19}$$

where

$$\Upsilon(r) \equiv 27\lambda_3^4 - 4\lambda_2^3\lambda_3^2 r^6 + 18\lambda_2\lambda_3^3 r^6 - \lambda_2^2\lambda_3^2 r^{12} + 4\lambda_3^3 r^{12},$$
$$\Sigma(r) \equiv 27\lambda_3^2 - 2\lambda_2^3 r^6 + 9\lambda_2\lambda_3 r^6, \tag{A20}$$

and where we set $r_0 = 1$ in all expressions.[7] The region in parameter space for which asymptotically flat black holes exist is displayed in Fig. 5. Whenever

$$-\frac{1 + 2\lambda_3}{\sqrt{2 + \lambda_3}} < \lambda_2 \quad \text{and} \quad \lambda_3 \leq 1, \tag{A21}$$

[7]This can be easily reintroduced by replacing $\lambda_2 \to \lambda_2/r_0^2$ and $\lambda_3 \to \lambda_3/r_0^4$.

there exists a black hole with a single horizon at

$$r_{\rm h} = \sqrt{\frac{-\lambda_2 + \sqrt{4 + \lambda_2^2 - 4\lambda_3}}{2}}. \tag{A22}$$

In particular, when

$$-\frac{1 + 2\lambda_3}{\sqrt{2 + \lambda_3}} < \lambda_2 \quad \text{and} \quad \lambda_3 < 0, \tag{A23}$$

the solution is described by $f_C(r)$ above and there is a finite-volume singularity at

$$r_\star \equiv \left(\frac{-2\lambda_2^3 + 2(\lambda_2^2 - 3\lambda_3)^{3/2} + 9\lambda_2\lambda_3}{\lambda_2^2 - 4\lambda_3}\right)^{1/6}. \tag{A24}$$

In addition, when

$$-\frac{1 + 2\lambda_3}{\sqrt{2 + \lambda_3}} < \lambda_2 < -\sqrt{3\lambda_3} \quad \text{and} \quad 0 < \lambda_3, \tag{A25}$$

the solution is described by $f_B(r)$ and there is a finite-volume singularity at $r_\star$. Finally, when

$$0 \le \lambda_3 < 1 \quad \text{and} \quad -\sqrt{3\lambda_3} < \lambda 2, \tag{A26}$$

the solution is described by $f_A(r)$ and it contains a singularity at $r = 0$.

When

$$1 < \lambda_3 < 4 \quad \text{and} \quad -\sqrt{3\lambda_3} < \lambda_2 < -2\sqrt{\lambda_3 - 1}, \tag{A27}$$

the solution is described by $f_A(r)$, and it contains a Cauchy horizon and an event horizon, respectively, at

$$r_{h_C} = \sqrt{\frac{-\lambda_2 - \sqrt{4 + \lambda_2^2 - 4\lambda_3}}{2}},$$
$$r_h = \sqrt{\frac{-\lambda_2 + \sqrt{4 + \lambda_2^2 - 4\lambda_3}}{2}}, \tag{A28}$$

and a singularity at $r = 0$.

[1] S. W. Hawking and G. F. R. Ellis, *The Large Scale Structure of Space-Time*, Cambridge Monographs on Mathematical Physics (Cambridge University Press, Cambridge, England, 2023), p. 2.

[2] V. A. Belinsky, I. M. Khalatnikov, and E. M. Lifshitz, Oscillatory approach to a singular point in the relativistic cosmology, Adv. Phys. **19**, 525 (1970).

[3] G. 't Hooft and M. J. G. Veltman, One loop divergencies in the theory of gravitation, Ann. Inst. Henri Poincare Phys. Theor. A **20**, 69 (1974).

[4] M. H. Goroff and A. Sagnotti, The ultraviolet behavior of Einstein gravity, Nucl. Phys. **B266**, 709 (1986).

[5] D. J. Gross and J. H. Sloan, The quartic effective action for the heterotic string, Nucl. Phys. **B291**, 41 (1987).

[6] M. T. Grisaru and D. Zanon, σ model superstring corrections to the Einstein-Hilbert action, Phys. Lett. B **177**, 347 (1986).

[7] A. D. Sakharov, Vacuum quantum fluctuations in curved space and the theory of gravitation, Dokl. Akad. Nauk SSSR **177**, 70 (1967).

[8] M. Visser, Sakharov's induced gravity: A modern perspective, Mod. Phys. Lett. A **17**, 977 (2002).

[9] S. Endlich, V. Gorbenko, J. Huang, and L. Senatore, An effective formalism for testing extensions to general relativity with gravitational waves, J. High Energy Phys. 09 (2017) 122.

[10] A. Frenkel, S. A. Hartnoll, J. Kruthoff, and Z. D. Shi, Holographic flows from CFT to the Kasner universe, J. High Energy Phys. 08 (2020) 003.

[11] S. A. Hartnoll, G. T. Horowitz, J. Kruthoff, and J. E. Santos, Gravitational duals to the grand canonical ensemble abhor Cauchy horizons, J. High Energy Phys. 10 (2020) 102.

[12] R.-G. Cai, L. Li, and R.-Q. Yang, No inner-horizon theorem for black holes with charged scalar hairs, J. High Energy Phys. 03 (2021) 263.

[13] S. A. H. Mansoori, L. Li, M. Rafiee, and M. Baggioli, What's inside a hairy black hole in massive gravity?, J. High Energy Phys. 10 (2021) 098.

[14] E. Caceres, A. Kundu, A. K. Patra, and S. Shashi, Trans-IR flows to black hole singularities, Phys. Rev. D **106**, 046005 (2022).

[15] M. Mirjalali, S. A. Hosseini Mansoori, L. Shahkarami, and M. Rafiee, Probing inside a charged hairy black hole in massive gravity, J. High Energy Phys. 09 (2022) 222.

[16] L.-L. Gao, Y. Liu, and H.-D. Lyu, Internal structure of hairy rotating black holes in three dimensions, J. High Energy Phys. 01 (2024) 063.

[17] M. De Clerck, S. A. Hartnoll, and J. E. Santos, Mixmaster chaos in an AdS black hole interior, J. High Energy Phys. 07 (2024) 202.

[18] D. Areán, H.-S. Jeong, J. F. Pedraza, and L.-C. Qu, Kasner interiors from analytic hairy black holes, arXiv:2407.18430.

[19] R.-G. Cai, M.-N. Duan, L. Li, and F.-G. Yang, Clarifying Kasner dynamics inside anisotropic black hole with vector hair, arXiv:2408.06122.

[20] L. Susskind, Computational complexity and black hole horizons, Fortschr. Phys. **64**, 24 (2016); **64**, 44(A) (2016).

[21] D. Stanford and L. Susskind, Complexity and shock wave geometries, Phys. Rev. D **90**, 126007 (2014).

[22] A. R. Brown, D. A. Roberts, L. Susskind, B. Swingle, and Y. Zhao, Holographic complexity equals bulk action?, Phys. Rev. Lett. **116**, 191301 (2016).

[23] P. Bueno, P. A. Cano, and R. A. Hennigar, Kasner epochs, eras and eons, Phys. Rev. D **110**, L041503 (2024).
[24] P. Bueno, P. A. Cano, and R. A. Hennigar, Regular black holes from pure gravity, arXiv:2403.04827.
[25] R. A. Konoplya and A. Zhidenko, Infinite tower of higher-curvature corrections: Quasinormal modes and late-time behavior of D-dimensional regular black holes, Phys. Rev. D **109**, 104005 (2024).
[26] F. Di Filippo, I. Kolář, and D. Kubiznak, Inner-extremal regular black holes from pure gravity, arXiv:2404.07058.
[27] R. A. Konoplya and A. Zhidenko, Dymnikova black hole from an infinite tower of higher-curvature corrections, Phys. Lett. B **856**, 138945 (2024).
[28] T.-X. Ma and Y.-Q. Wang, Frozen boson stars in an infinite tower of higher-derivative gravity, arXiv:2406.08813.
[29] N. Deruelle, On the approach to the cosmological singularity in quadratic theories of gravity: The Kasner regimes, Nucl. Phys. **B327**, 253 (1989).
[30] T. Clifton and J. D. Barrow, Further exact cosmological solutions to higher-order gravity theories, Classical Quantum Gravity **23**, 2951 (2006).
[31] J. Middleton, On the existence of anisotropic cosmological models in higher-order theories of gravity, Classical Quantum Gravity **27**, 225013 (2010).
[32] M. de Cesare and E. Wilson-Ewing, A generalized Kasner transition for bouncing Bianchi I models in modified gravity theories, J. Cosmol. Astropart. Phys. 12 (2019) 039.
[33] S. Deser and B. Tekin, Shortcuts to high symmetry solutions in gravitational theories, Classical Quantum Gravity **20**, 4877 (2003).
[34] R. S. Palais, The principle of symmetric criticality, Commun. Math. Phys. **69**, 19 (1979).
[35] P. Bueno and P. A. Cano, Universal black hole stability in four dimensions, Phys. Rev. D **96**, 024034 (2017).
[36] G. Arciniega, P. Bueno, P. A. Cano, J. D. Edelstein, R. A. Hennigar, and L. G. Jaime, Geometric inflation, Phys. Lett. B **802**, 135242 (2020).
[37] P. Bueno, P. A. Cano, and R. A. Hennigar, (Generalized) quasi-topological gravities at all orders, Classical Quantum Gravity **37**, 015002 (2020).
[38] P. Bueno, P. A. Cano, V. S. Min, and M. R. Visser, Aspects of general higher-order gravities, Phys. Rev. D **95**, 044010 (2017).
[39] X. O. Camanho, N. Dadhich, and A. Molina, Pure Lovelock Kasner metrics, Classical Quantum Gravity **32**, 175016 (2015).
[40] D. Lovelock, The Einstein tensor and its generalizations, J. Math. Phys. (N.Y.) **12**, 498 (1971).
[41] D. Lovelock, The four-dimensionality of space and the Einstein tensor, J. Math. Phys. (N.Y.) **13**, 874 (1972).
[42] D. G. Boulware and S. Deser, String generated gravity models, Phys. Rev. Lett. **55**, 2656 (1985).
[43] J. T. Wheeler, Symmetric solutions to the Gauss-Bonnet extended Einstein equations, Nucl. Phys. **B268**, 737 (1986).
[44] R. C. Myers and J. Z. Simon, Black hole thermodynamics in Lovelock gravity, Phys. Rev. D **38**, 2434 (1988).
[45] J. de Boer, M. Kulaxizi, and A. Parnachev, Holographic Lovelock gravities and black holes, J. High Energy Phys. 06 (2010) 008.
[46] X. O. Camanho and J. D. Edelstein, A Lovelock black hole bestiary, Classical Quantum Gravity **30**, 035009 (2013).
[47] T. Kitaura and J. T. Wheeler, Anisotropic, time dependent solutions in maximally Gauss-Bonnet extended gravity, Nucl. Phys. **B355**, 250 (1991).
[48] T. Kitaura and J. T. Wheeler, New singularity in anisotropic, time dependent, maximally Gauss-Bonnet extended gravity, Phys. Rev. D **48**, 667 (1993).
[49] E. J. Martinec, Space-like singularities and string theory, Classical Quantum Gravity **12**, 941 (1995).
[50] Y. Zigdon, Stringy forces in the black hole interior, J. High Energy Phys. 11 (2024) 063.
[51] N. Graham and K. D. Olum, Achronal averaged null energy condition, Phys. Rev. D **76**, 064001 (2007).
[52] R.-G. Cai, S.-M. Ruan, S.-J. Wang, R.-Q. Yang, and R.-H. Peng, Action growth for AdS black holes, J. High Energy Phys. 09 (2016) 161.
[53] P. A. Cano, R. A. Hennigar, and H. Marrochio, Complexity growth rate in Lovelock gravity, Phys. Rev. Lett. **121**, 121602 (2018).
[54] R. Emparan, A. M. Frassino, M. Sasieta, and M. Tomašević, Holographic complexity of quantum black holes, J. High Energy Phys. 02 (2022) 204.
[55] P. A. Cano, R. A. Hennigar, and H. Marrochio (unpublished).
[56] E. Cáceres, A. J. Murcia, A. K. Patra, and J. F. Pedraza, Kasner eons with matter: Holographic excursions to the black hole singularity, arXiv:2408.14535.